

# Patterning of Sol–Gel Hybrid Organic–Inorganic Film Doped with Luminescent Semiconductor Quantum Dots

Dario Buso<sup>1</sup>, Gioia Della Giustina<sup>1</sup>, Giovanna Brusatin<sup>1</sup>, Massimo Guglielmi<sup>1</sup>,  
Alessandro Martucci<sup>1,\*</sup>, Alessandro Chiasera<sup>2</sup>, Maurizio Ferrari<sup>2</sup>, and Filippo Romanato<sup>3</sup>

<sup>1</sup> Dipartimento di Ingegneria Meccanica–Settore Materiali, Università di Padova, via Marzolo 9, 35131 Padova, Italy

<sup>2</sup> CNR-IFN Istituto di Fotonica e Nanotecnologie, via Sommarive 14, 38050 Povo Trento, Italy

<sup>3</sup> Lab. TASC of INFN-CNR, 34012 Basovizza-Trieste, Italy also at Institute of Material Science and Technology, Nanyang Technological University, Singapore, 639798

Two different sol–gel hybrid organic–inorganic films doped with luminescent CdS or PbS quantum dots (QDs) have been successfully synthesized and patterned using nanolithographic techniques. The feasibility of applying X-ray lithography and RIE to pattern hybrid materials doped with highly luminescent nanoparticles has been demonstrated for GPTMS-GeO<sub>2</sub> (G-GeO<sub>2</sub>) and MPTMS-ZrO<sub>2</sub> (M-ZrO<sub>2</sub>) hybrids obtained from 3-glycidioxypropyltrimethoxysilane (GPTMS), methacryloxy-propyltrimethoxysilane (MPTMS), germanium ethoxide and zirconium propoxide. Semiconductor doped film have been obtained by mixing ZrO<sub>2</sub>-SiO<sub>2</sub> or GeO<sub>2</sub>-SiO<sub>2</sub> sol–gel hybrid organic–inorganic matrix solution with CdS or PbS colloidal doping solution to obtain up to 20% molar concentration of QDs inside the films. Patterns consisting of pillars with different aspect ratio have been obtained by X-ray lithography and reactive ion etching (RIE). Structural and optical characterization of films before and after the lithographic process pointed out that both matrices and QDs retain their original properties without been affected by X-rays irradiation and RIE in the conditions here described.

**Keywords:** Sol–Gel, Hybrid, Film, Quantum Dots, Patterning, X-ray Lithography.

## 1. INTRODUCTION

Photolithographic strategies are among the most widely adopted industrial microfabrication techniques and represent a fundamental building block in the modern microelectronics market. The current overlap between electronics and photonics leads to the need of design new optically active structures that can be easily implemented in industrial techniques. Photolithography is currently an indispensable contributor to information technology (i.e., fabrication of sensors, microreactors, micro-optical and microanalytical systems).<sup>1</sup> A promising approach is given by using photolithography on innovative materials that could constitute the ultimate material of the device to perform. Among these materials hybrids matrices obtained by sol–gel offer an outstanding range of properties and compositions by combining inorganic and organic components that extend the possible range of applications and performances of integrated optic devices. In fact, the introduction of organic groups into an inorganic network structure enables the hybrid sol gel glasses to tailor their

chemical and physical properties (improved mechanical properties, low densification temperature, tailored refractive index, etc.). The sol–gel process is a chemical solution deposition method whose many advantages lie in atomic level mixing of high purity of starting materials, high versatility, low processing temperature and low cost. In addition, the sol–gel materials are compatible with planar integrated optics technology, they are chemically and mechanically robust and their optical quality is high and widely tunable.

Nanocrystalline Quantum Dots (QDs) are colloidal synthesized nanometer-sized particles of binary semiconductors such as CdS, CdSe, or ZnSe, exhibiting bulk bonding structure<sup>2</sup> and giving a series of discrete optical transitions corresponding to different quantum-confined electron and hole states.<sup>3</sup> Quantum confinement leads to strongly size-dependent optical properties,<sup>4</sup> making them attractive candidates for use in a wide range of optoelectronic devices where the absorption or emission may be tuned through control of the nanocrystal size. Significant potential for serving as luminescent chromophores are addressed to applications ranging from lasers<sup>5</sup> and optoelectronic devices,<sup>6</sup> to biological fluorescence tagging.<sup>7,8</sup>

\*Author to whom correspondence should be addressed.

Applications in optics require the optical information or signal to be transmitted with high propagation efficiency, so embedding the nanocrystals into a solid matrix becomes a leading target. Few papers have been published on patterned film doped with semiconductor quantum dots.<sup>9,10</sup> Aim of this work is the synthesis of hybrid organic-inorganic glass film doped with CdS (emitting in the visible) and PbS (emitting in the near infrared) quantum dots which retains their optical properties after nanopatterning.

## 2. EXPERIMENTAL DETAILS

### 2.1. Material Synthesis

#### 2.1.1. Synthesis of Sol Gel G-GeO<sub>2</sub> Matrix

3-glycidioxypropyl-trimethoxysilane (GPTMS) was first mixed with H<sub>2</sub>O according to H<sub>2</sub>O:GPTMS = 3:1 (molar) and let hydrolyze overnight under constant stirring. A 1:2 molar mixture of germanium tetra-ethoxide (TEOG) and H<sub>2</sub>O was then added to the GPTMS solution to get a GPTMS:TEOG = 7:3 molar ratio. The overall solution batch was kept at reflux condition (~80 °C) for 1 h 30 min in a slightly basic environment obtained by means of NaOH addition (0.3% molar respect to GPTMS). The final (SiO<sub>2</sub> + GeO<sub>2</sub>) concentration was tailored to 150 g/L by addition of 2-methoxy-ethanol as solvent.

#### 2.1.2. Synthesis of Sol Gel M-ZrO<sub>2</sub> Matrix

Hydrolysis of metacryloxy-propyl-trimethoxysilane (MPTMS) was promoted by a H<sub>2</sub>O/HCl mixture under constant stirring for 1 h according to MPTMS:H<sub>2</sub>O:HCl = 1:1:0.0075 molar ratios using 1 M HCl. Separately a solution of zirconium propoxide and methacrylic acid (MA) was let stirring for 1h to promote an effective chelation of the zirconium precursor. Global molar ratios were MPTMS:Zr:MA = 1:0.57:0.23. The two solutions were then mixed and let stirring for further 45 minutes before a final amount of water was added to get a (MPTMS + Zr):H<sub>2</sub>O = 1:0.08 molar ratio and let react for 90 minutes before films deposition.

#### 2.1.3. Synthesis of CdS QDs

A solution of cadmium acetate dihydrate (CdAc) in methanol containing mercaptopropyl-trimethoxysilane (MTMS:CdAc = 2:1) was mixed with a thioacetamide (TAA) solution in methanol (TAA:CdAc = 1:1) at room temperature. CdS nanocrystals growth was promoted increasing the temperature to 60 °C under constant stirring for 20 minutes. The initial concentration of CdAc was tailored to get molar contents of QDs inside the final films of 5% and 20%.

#### 2.1.4. Synthesis of PbS QDs

Lead acetate (PbAc) was dissolved in methanol in presence of acetic acid (HAc) and MTMS according to PbAc:HAc:MTMS = 1:4.75:2 molar ratios. A separately prepared solution of TAA in methanol (TAA:PbAc = 1:1) was then added at room temperature and PbS nanocrystals growth observed immediately with no need of heating. Initial amount of PbAc was designed to obtain a final PbS molar content in films of 5% and 20%.

#### 2.1.5. Synthesis of Hybrid Sol Gel Films Containing QDs

A common procedure was employed in the realization of the final sol gel solutions containing both the hybrid matrices precursors and the QDs. The initial sol gel sols were mixed with the QDs doping suspensions according to 1:1 volume ratio in all cases. QDs contents in sol gel sols were controlled simply tailoring the nanoparticles concentration in the starting QDs suspensions. Films were deposited on silica glass or silicon substrates spin coating the final sol gel solution at 2000 rpm for 30 seconds in the case of CdS doped matrices and at 1200 rpm for 30 seconds for PbS doped ones. Samples underwent thermal annealing at 120 °C for 2 hours in order to further promote the inorganic network condensation and polymerization of the organic phase.

All chemicals were purchased from Aldric.

### 2.2. Lithographic Process

The lithographic print was performed using soft X radiation at around 1.5 keV from the LILIT beamline at ELETTRA Synchrotron Light Source in Trieste, Italy.<sup>11</sup> Pure commercial SAL was used as negative photoresist. In order to optimize the adhesion between SAL and sol gel films a sacrificial PMMA layer was first spin coated on the films surface. Commercial PMMA 671.01 solution was deposited at 4000 rpm for 30 seconds and the ~50 nm thick PMMA layer let polymerize for 10 minutes at 175 °C. Subsequently pure SAL was spin coated on the PMMA layer at 4000 rpm for 30 seconds and pre-baked at 105 °C for 1 minute. The deposited SAL film resulted to be 800 nm thick. The samples were then covered with especially designed masks and exposed to the X-rays beam using an irradiation dosage of 165 mJ/cm<sup>2</sup>. Exposed films underwent a post-baking step at 105 °C for 75 seconds and then developed for 3 minutes using MF-322 industrial developer. Reacting Ion Etching (RIE) was performed using a 1:2 volumetric mixture flux of Argon and CF<sub>4</sub> as plasma source generated with a cathode bias voltage of 440 V at 30 Pa. Residual SAL layer was then totally stripped away by means of hot acetone. The sacrificial PMMA layer previously deposited facilitated the complete removal of any resist traces on sol gel films' surface.

### 2.3. Material Characterizations

The crystalline phase of film doped with semiconductor quantum dots have been characterized by a Philips PW1710 X-ray diffraction (XRD) using a diffractometer equipped with grazing-incidence X-ray optics. The analysis was performed using  $\text{CuK}_\alpha$ -Ni filtered radiation at 40 kV and 40 mA. The average crystallite size was calculated using the Scherrer correlation after fitting the experimental profiles with a pseudo-Voigt function.

UV-Vis-NIR absorption spectra were taken using a JASCO V-570 spectrometer, performing the measurement at room temperature.

Photoluminescence properties have been investigated using a Xenon lamp in reflectance configuration exciting at 350 nm (CdS doped film) or at 514 nm (PbS doped film).

The films deposited on silicon were analyzed with Fourier Transform Infrared Spectroscopy (FTIR), and spectra were taken in the  $400\text{--}4000\text{ cm}^{-1}$  region using a resolution of  $2\text{ cm}^{-1}$ .

The waveguides properties of the films and their refractive index at 632.8 and at 543.5 nm were measured in TE and TM polarization by an *m*-line apparatus based on the prism coupling technique.

The patterned films have been characterized with a Philips scanning electron microscope (SEM) and optical microscope (Nikon).

## 3. RESULTS

Hybrid sol gel films doped with QDs resulted optically transparent and homogeneous in color. Figure 1 reports the absorbance spectra of both undoped and doped G-GeO<sub>2</sub> films containing CdS (a) and PbS (b) QDs. M-ZrO<sub>2</sub> films containing CdS and PbS nanoparticles showed similar absorption spectra (not reported for the seek of clarity). Both CdS doped matrices present typical absorbance spectra dominated by the semiconductor exciton peak at 378 nm for all CdS concentrations, noticeably blue shifted from the CdS bulk value (512 nm) demonstrating a quantum size confinement. CdS nanoparticles diameter can be estimated by the energy gap value<sup>14</sup> and resulted to be 2.75 nm. Even if the absorption spectra of PbS doped film consist of a long tail with no resolved sub-banding, we can see a large shift of the absorption edge to the high energy side relative to the bulk PbS ( $E_g = 3200\text{ nm}$ ), an effect that is representative of a quantum confinement effect. The absorption curves are featureless, i.e., no excitonic absorption structure can be observed. However, weak interference fringes are visible caused by the reflection at the film-air and film-substrate interfaces.

Films thickness and refractive indexes measured with *m*-line at 633 nm and 543.5 nm are reported in Table I. Thickness of G-GeO<sub>2</sub> films varies from about  $2\ \mu\text{m}$  for the undoped matrix to about  $1.5 \div 1.8\ \mu\text{m}$  for QDs

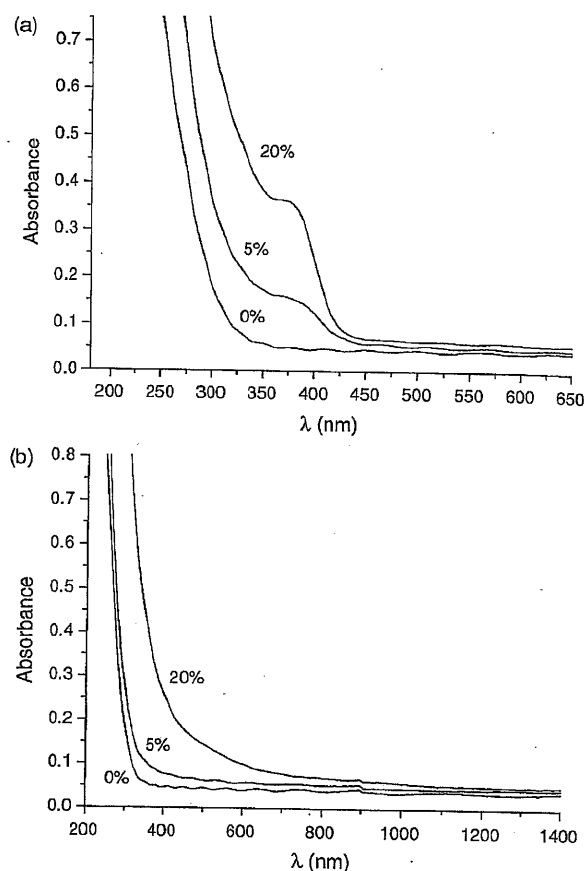


Fig. 1. Optical absorption spectra of (a) CdS and (b) PbS doped G-GeO<sub>2</sub> film. Molar concentration of QDs varies in the 0–20% range and is reported on the plot lines.

doped ones, presenting refractive indexes in the  $1.50 \div 1.53$  range. Higher refractive indexes are measured for higher QDs contents. Measured M-ZrO<sub>2</sub> films thickness resulted in the  $1.1 \div 1.5\ \mu\text{m}$  range with refractive indexes varying from 1.52 to 1.57 for higher QDs concentrations. Refractive index of all samples showed negligible variation throughout the films thickness (1% variation maximum),

Table I. Doped and undoped G-GeO<sub>2</sub> and M-ZrO<sub>2</sub> films thickness and refractive indexes measured with *m*-line.

Matrix	Dopant	Film thickness ( $\mu\text{m}$ )	Refractive index	
			@ 633 nm	@ 543.5 nm
G-GeO <sub>2</sub>	—	$2.2 \pm 0.1$	1.5019	—
	5% CdS	$1.5 \pm 0.1$	1.5048	1.5094
	20% CdS	$1.87 \pm 0.01$	1.5331	1.5386
	5% PbS	$1.5 \pm 0.1$	1.5022	—
	20% PbS	$1.7 \pm 0.1$	1.5349	—
M-ZrO <sub>2</sub>	—	$1.3 \pm 0.1$	1.5237	1.5277
	5% CdS	—	1.5339	1.5385
	20% CdS	$1.5 \pm 0.1$	1.5671	1.5750
	5% PbS	$1.1 \pm 0.1$	1.5309	1.5358
	20% PbS	$1.3 \pm 0.1$	1.5582	—

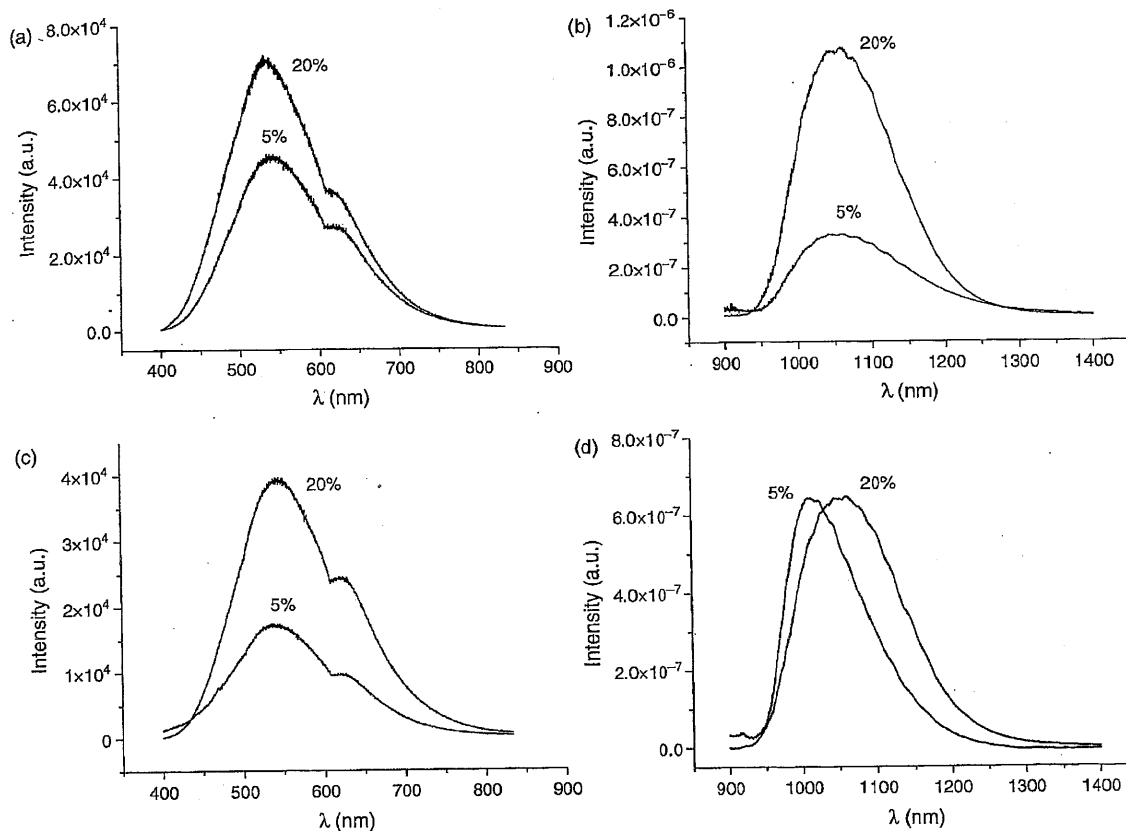


Fig. 2. Photoluminescence emission of (a) CdS, (b) PbS doped G-GeO<sub>2</sub> film and (c) CdS, (d) PbS doped M-ZrO<sub>2</sub> film. QDs concentrations are reported on each plot line. CdS QDs were excited at 350 nm while PbS QDs at 514 nm.

thus demonstrating good compositional homogeneity of materials in all cases.

Figure 2 shows emission spectra measured for QDs doped matrices. Figure 2(a) reports photoluminescence spectra of G-GeO<sub>2</sub> matrix doped with 5% and 20% of CdS nanoparticles, while Figure 2(c) shows emission raising from CdS QDs (5% and 20%) in M-ZrO<sub>2</sub> film. QDs doped films showed in all cases two broad bands centered at 540 nm and 630 nm. The emission intensity is dependent on the QDs concentration and on the matrix nature itself. At same CdS content in fact doped G-GeO<sub>2</sub> films showed a higher intensity emission if compared to the doped M-ZrO<sub>2</sub> matrices, but it must be taken into account that the former films are generally 300 nm thicker than the latter, thus being characterized by a higher absolute number of emitting particles.

PbS doped matrices showed photoluminescence spectra reported in Figures 2(b, d). Emission signals presented a wide peak centered at 1058 nm with exception for M-ZrO<sub>2</sub> doped with 5% PbS which emission peak is at 1015 nm, with intensities varying according to particles concentration and matrix nature. The overall photoluminescence extent is observed in the 900–1300 nm region. PbS QDs

in G-GeO<sub>2</sub> matrix show also in this case higher emission intensities.

XRD measurements showed the presence of CdS and PbS crystalline phases. In the case of CdS doped samples the diffraction peaks were very broad and it was not possible to assign the phase. On the contrary the PbS doped films showed well discernable diffractions peaks, which have been assigned to lead sulfide in the cubic phase. From the line broadening of the main diffraction peaks it was estimated a mean diameter of 3–4 nm.

FTIR spectra of both PbS doped and undoped matrices are shown in Figure 3. Similar spectra have been obtained for CdS doped matrices (not reported for the seek of clarity).

Contributions of OH groups are indicated by the broad band in the 3000–3700 cm<sup>-1</sup> region in all spectra, together with CH<sub>2</sub> and terminal CH<sub>3</sub> doublets around 2900 cm<sup>-1</sup> (2937 and 2872 cm<sup>-1</sup>).<sup>16</sup> Spectra in Figure 3(a) show the epoxy vibrations at 3060 and 3000 cm<sup>-1</sup> (Ref. [18]) in the GPTMS based matrix. The 800–1250 cm<sup>-1</sup> region presents vibrational signals raising from the SiO<sub>2</sub> network, mainly Si–O–Si stretching bonds, unreacted silanols, Si–O–C<sub>2</sub>H<sub>5</sub> and Si–CH<sub>2</sub>– contributions.<sup>16,17</sup> Signals

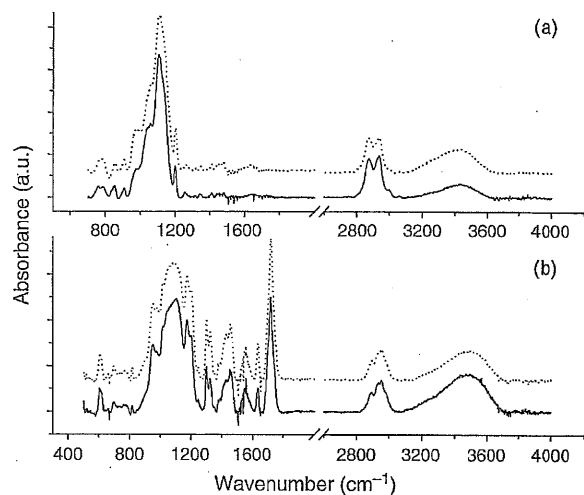


**Fig. 3.** FTIR spectra of (a) PbS doped G-GeO<sub>2</sub> film and (b) PbS doped M-ZrO<sub>2</sub>. Each panel reports a spectrum of undoped matrix (dot line) and a spectrum of the same film containing 20% of QDs (solid line).

related to carboxyl terminations and to polymerized methacrylate groups are evident in the 1200–1700 cm<sup>-1</sup> range in Figure 3(b) spectra.

SEM pictures reported in Figure 4 show some of the patterned structure obtained on sol gel hybrid matrices doped with CdS and PbS QDs. Images taken after residual resist stripping, subsequent to RIE process, show the final structures impressed in hybrid doped sol gel films. The obtained structures are well resolved in a depth of about 750 nm, with the only drawback of the roughness of the etched area. Optimization of etching parameters will be effective in further smoothing of the etched surface.

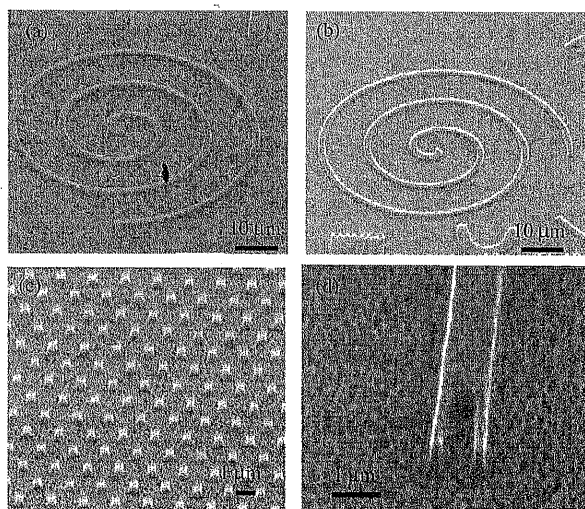


**Fig. 4.** SEM images of some of the patterned geometries obtained on G-GeO<sub>2</sub> matrix doped with CdS or PbS QD. (a) and (b) show a spiral structure doped with 20% CdS and 20% PbS respectively. (c) Periodic vertical pillars (750 nm high) doped with 20% PbS. (d) Elongated shapes from a film doped with 5% CdS. The scale unit for (a) and (b) is 10 μm and 1 μm in (c) and (d).

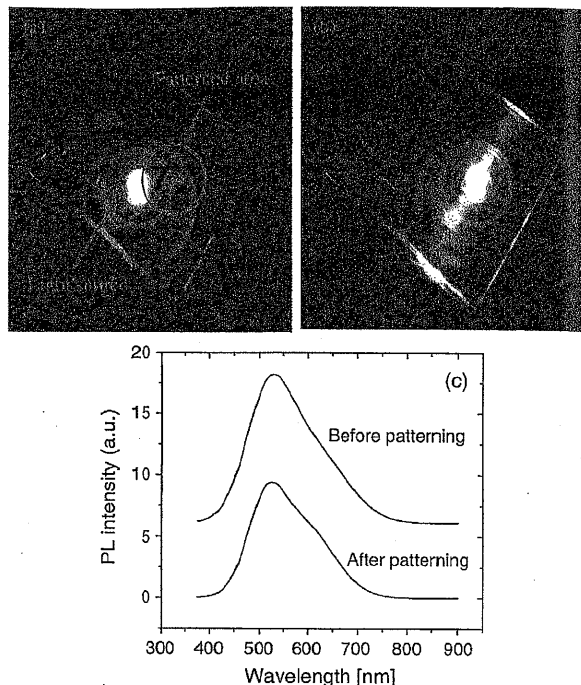


**Fig. 5.** Pictures of a M-ZrO<sub>2</sub> film doped with 5% CdS and patterned with a 350 nm deep Bragg diffraction grid. The pattern, indicated in (a) by a red circle, is made of parallel channels 500 nm wide and 500 spaced. (b) Shows the effect of a coupled light source in the film. Photoluminescence spectra of the same film before and after patterning is also reported.

Pictures in Figure 5 show the effect of a Bragg diffraction grid patterned on a M-ZrO<sub>2</sub> film doped with 5% CdS QDs. The pattern, indicated in Figure 5(a) by the red circle, consists of parallel channels 500 nm spaced, 500 nm wide and 350 nm deep. Figure 5(b) show the effect of a coupled light source (a simple transmission microscope light source) in the film thickness. The perpendicular light beam is deviated in the direction of the channels and coupled perpendicularly in the higher refractive index layer.

#### 4. DISCUSSION

The absence of a narrow and resolved exciton peak in the optical absorption spectra rising from QDs indicates that the nanoparticles sizes are distributed in a wide range of values. While CdS QDs mean diameter was estimated to be 2.75 nm, the evaluation of PbS nanocrystals mean dimension is made difficult by the absolute absence of an exciton peak in the absorption spectra. XRD measurements indicate for PbS nanoparticles a mean diameter of 3–4 nm. In previous papers<sup>18,19</sup> we showed that the use of amino or mercapto silanes as surface capping agent allow homogeneous dispersion of semiconductor nanoparticles in sol-gel film.

The two broad bands in the photoluminescence spectra of CdS doped film (Figs. 2(a and c)) can be assigned to

band-edge luminescence (band at 540 nm) and to recombination at defects (band at 630 nm).<sup>20</sup>

The single emission peak observed for PbS doped film in the near infrared region is in good agreement with other published photoluminescence spectra of PbS nanoparticles in sol-gel film.<sup>13,21</sup> The Gaussian shape of the photoluminescence emission peaks suggest inhomogeneous broadening related to the size dispersion and/or recombination through surface states.

The process to obtain patterned structures on sol-gel matrices optically activated by introduction of luminescent nanoparticles is an example of successful synergy between chemistry, physical chemistry and engineering as a starting point for the realization of a functional device. Semiconductors QDs potentiality in functional solid state devices has not been exploited extensively yet, as nowadays the QDs market mainly stands on liquid state biological labeling and DNA sequences identification.<sup>7,8</sup>

A successful embedding and stabilization of high quantities of QDs in a sol gel matrix is achieved with a proper control of the nanoparticles surface chemistry. MPTMS is known to be effective to stabilize high QDs amounts in hybrid matrices<sup>13</sup> retaining their optical properties. It was also found that acidic environments are detrimental for the structural stability of QDs, as it was observed that they undergo chemical etching at low pHs. In this condition a systematic desorption of capping agent molecules from the QDs surface is favored by protonation of the surfactant molecules' head groups that are adsorbed on the QDs surface. An optimized surface stability is thus a key factor to maintain optical characteristics of QDs inside the hosting matrix.<sup>12</sup> This could explain why the G-GeO<sub>2</sub> matrix, based on a slightly basic sol gel solution, seems to confer higher luminescence intensities to embedded QDs, both CdS and PbS, while the emission intensity of the same species hosted in the more acidic M-ZrO<sub>2</sub> matrix results partially inhibited. Moreover FTIR signals rising from polymerized methacrylate network testify that a reaction process via radicals' addition occurred during the thermal annealing of samples. These reactive groups can effectively promote some of the capping agent molecules decomposition, thus increasing the overall number of non-radiative recombination centers on QDs surfaces as it was observed after annealing at higher temperatures (up to 200 °C), i.e., after promoting a complete polymerization of the methacrylate network.

5% PbS in M-ZrO<sub>2</sub> seem to particularly suffer this matrix effects, as blue shift in the absorbance edge and luminescence intensity maximum indicate that QDs in this conditions are smaller in size if compared to 5% PbS in G-GeO<sub>2</sub>. It must be considered that PbS QDs came from the same reaction batch.

FTIR analysis was useful to confirm that no substantial structural modification of matrices was induced by QDs doping. No appreciable differences in peak signals or trend

with nanoparticles concentration were observed. This further accentuates the enhancing role that QDs play in films refractive indexes as pointed out in Table I. In this case a trend with QDs content is evident.

SEM images of Figure 4 demonstrates the feasibility of a lithographic process to create desired shaped structures in micrometric layers derived from the above described sol gel solutions. It was observed that the patterned structures adhere strongly to the substrate and can be moulded in sub-micrometric three dimensional geometries with high control and reproducibility, essential requirements for large scale applications. The obtained structures are well resolved and show a depth of about 750 nm, easily increasable with longer RIE treatments.

Pictures in Figure 5 demonstrate the effectiveness of the above described Bragg diffraction pattern to couple a light source into the film thickness in the same direction of the channels. The coupled light is in this simple case sufficient to stimulate the green emission of embedded CdS QDs. Emission spectra reported in the same figure testifies that the optical quality of QDs remains fairly unaltered by the lithographic procedure. The substantially unvaried emission peak maximum wavelength and shape permit to conclude that the nanocrystals structural morphology has not changed.<sup>15</sup>

## 5. CONCLUSIONS

A successful embedding of CdS and PbS QDs inside high refractive index hybrid GPTMS-GeO<sub>2</sub> and MTPMS-ZrO<sub>2</sub> sol gel matrices has been carried out. The QDs surface chemistry control allowed to stabilize the nanoparticles inside the hosting networks at molar concentrations up to 20% and to retain their optical properties once embedded. A tailored lithographic process was performed in order to pattern the sol gel doped matrices with some simple three dimensional geometries and study the effects of this procedure on the matrices structure and optical properties. The films demonstrate to be mechanically resistant to the patterning pathway and hosted QDs showed to retain effectively their morphological microstructure and consequently their optical properties.

**Acknowledgments:** This work has been supported by MIUR through PRIN 2006 research project and the FIRB Italian project RBNE033KMA 'Molecular compounds and hybrid nanostructured materials with resonant and non resonant optical properties for photonic devices.'

## References and Notes

1. C. R. Barrett, *Mat. Res. Soc. Bull.* 18, 3 (1993).
2. A. P. Alivisatos, *J. Phys. Chem.* 100, 13226 (1996).
3. D. J. Norris and M. G. Bawendi, *Phys. Rev. B* 53, 16338 (1996).
4. A. D. Yoffe, *Adv. Phys.* 42, 216 (1993).

5. V. I. Klimov, A. A. Mikhailovsky, S. Xu, J. A. Hollingsworth, C. A. Leatherdale, H. J. Bisler, and M. G. Bawendi, *Science* 290, 314 (2000).
6. V. L. Colvin, M. C. Schlamp, and A. P. Alivisatos, *Nature* 370, 354 (1994).
7. M. P. Bruchez, M. Moronne, P. Gin, S. Weiss, and A. P. Alivisatos, *Science* 281, 2013 (1998).
8. W. C. W. Chan and S. Nie, *Science* 281, 2016 (1998).
9. M. F. Bertino, R. R. Gadipalli, L. A. Martin, L. E. Rich, A. Yamilov, B. R. Heckman, N. Leventis, S. Guha, J. Katsoudas, R. Divan, and D. C. Mancini, *Nanotechnology* 18, 315683 (2007).
10. M. Tamborra, M. Striccoli, M. L. Curri, J. A. Alducin, D. Mecerreyes, J. A. Pomposo, N. Kehagias, V. Reboud, C. M. Sotomayor Torres, and A. Agostiano, *Small* 3, 822 (2007).
11. F. Romanato, E. Di Fabrizio, L. Vaccari, M. Altissimo, D. Cojoc, L. Businaro, and S. Cabrini, *Microelectron. Eng.* 101, 57 (2001).
12. W. W. Yu, L. H. Qu, W. Z. Guo, and X. G. Peng, *Chem. Mater.* 15, 2854 (2003).
13. A. Martucci, J. Fick, S. E. LeBlanc, M. LoCascio, and A. Hache, *J. Non-Cryst. Solids* 345, 639 (2004).
14. S. T. Selvan, C. Bullen, M. Ashokkumar, and P. Mulvaney, *Adv. Mater.* 13, 985 (2001).
15. S. F. Wuister and A. Meijerink, *J. Luminescence* 102-103, 338 (2003).
16. G. Brusatin, G. Della Giustina, M. Guglielmi, and P. Innocenzi, *Prog. Sol. State Chem.* 34, 223 (2006).
17. P. Innocenzi, M. O. Abdirashid, and M. Guglielmi, *J. Sol-Gel Sci. Tech.* 3, 47 (1994).
18. A. Martucci, P. Innocenzi, J. Fick, and J. D. Mackenzie, *J. Non-Crystalline Solids* 55-62, 244 (1999).
19. C. Bullen, P. Mulvaney, C. Sada, M. Ferrari, and A. Martucci, *J. Mater. Chemistry* 1112-1116, 14 (2004).
20. T. R. Ravindran, A. K. Arora, B. Balamurugan, and B. R. Mehta, *Nanostruct. Mater.* 11, 603 (1999).
21. A. Sashchiuk, E. Lifshitz, R. Reinfeld, T. Saraidarov, M. Zelner, and A. Willenz, *J. Sol-Gel Sci. Tech.* 24, 31 (2002).

Received: 16 January 2008. Accepted: 6 March 2008.